

Specific Interactions in the Inclusion Complexes of Pyronines Y and B with  $\beta$ -Cyclodextrin

Belén Reija, Wajih Al-Soufi, Mercedes Novo,\* and José Vázquez Tato

*Departamento de Química Física, Facultade de Ciencias,  
Universidade de Santiago de Compostela, E-27002 Lugo, Spain**Received: July 30, 2004; In Final Form: October 29, 2004*

The aim of this work is to analyze the role of specific interactions in host–guest association processes. The formation of inclusion complexes between pyronines Y and B and  $\beta$ -cyclodextrin and the nature of the interactions involved have been studied using absorption, steady-state fluorescence, and time-resolved fluorescence spectroscopies. The two pyronines form 1:1 complexes with  $\beta$ -cyclodextrin, with the association equilibrium constant being much higher in the case of pyronine B. Complexation causes a slight red shift of the emission spectra of the pyronines but decreases significantly their fluorescence quantum yields and lifetimes. To explain this atypical behavior, the photophysical properties of the pyronines in different solvents were determined and compared with those of the complexes. The similarities observed between the pyronines in dioxane and in the interior of the cyclodextrin cavity suggest that there are important specific interactions of the pyronines with the electron-rich oxygens present in these media. A possible explanation for the increase in the nonradiative rate constants in these media involves the existence of a charge-transfer excited state with the location of the positive charge at the xanthene moiety, which would be stabilized by the mentioned interactions. The observed differences between pyronine Y and B can be understood on the basis of these specific interactions.

## Introduction

Pyronines Y (PY) and B (PB) are cytotoxic dyes used in the Unna Pappenheim stain for ribonucleic acid (Figure 1). They provide simplified models of the xanthene skeleton of rhodamines, which are also used in the labeling of proteins and cell organelles. For these applications, it is important to understand the photophysical behavior of the dyes in organized media and to know the role of the interaction between the substrate and the medium. Cyclodextrins (CDs), which are toroidally shaped polysaccharides with a highly hydrophobic central cavity, are good model systems due to their ability to form inclusion complexes with many organic substrates. The specific non-covalent interactions between CDs and guest molecules resemble those controlling molecular recognition phenomena in biological systems.<sup>1</sup>

When compared to rhodamines, pyronines have similar photophysical properties which are much influenced by the aggregation of the dyes.<sup>2–4</sup> However, the lack of a substituent at the C9 position of the xanthene ring allows reversible hydrolysis of pyronine cations into the corresponding xanthydrols, which show blue-shifted fluorescence.<sup>2,5</sup> Even in basic media, this process is quite slow, but it is responsible for the observed chemical instability of pyronines in aqueous solution. Comparing the two pyronines under study, PB shows much higher reactivity with water than PY, which is more stable.

The ability of PY and PB to form inclusion complexes with CDs has been reported by Schiller et al.<sup>6–8</sup> The authors used visible absorption spectra to determine the complexation equilibrium constants and temperature-jump spectrophotometry to study the kinetics of the association/dissociation processes. Nevertheless, the experimental data presented do not clearly support the proposed models and strong assumptions in the data

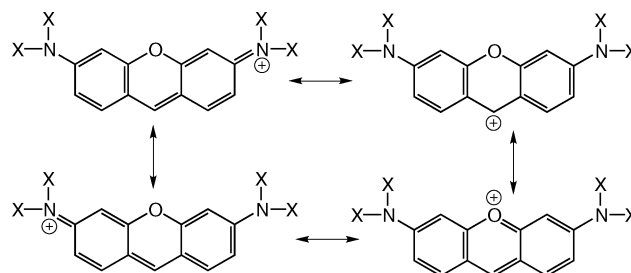


**Figure 1.** Resonance structures of the pyronines used in this work, with X = CH<sub>3</sub> for PY and X = CH<sub>2</sub>CH<sub>3</sub> for PB.

analysis were made. Moreover, experimental conditions were chosen in order to favor the formation of pyronine aggregates.

In this work, we study the complexation of PY and PB with  $\beta$ -cyclodextrin ( $\beta$ -CD) using, together with ultraviolet–visible (UV–vis) absorption, the more sensible techniques of steady-state and time-resolved fluorescence. The aim of the study is to characterize the photophysical properties of these pyronines when included in the hydrophobic cavity of  $\beta$ -CD, to discuss the guest–host interactions involved in the formation of the complexes.

## Experimental Section

**Materials.** PY was purchased from Sigma (51% dye content) and PB from Aldrich (57% dye content). The main impurities of these materials are not water soluble, so that they can be separated by filtration of the aqueous solutions.<sup>7</sup>  $\beta$ -cyclodextrin (kindly supplied by Roquette) was recrystallized twice from water and dried in a vacuum oven. HClO<sub>4</sub> (Merck, p.a.) was used to control the pH of the solutions. Water was purified with a Milli-Q system. The organic solvents were all of HPLC grade, and the absence of fluorescent impurities was checked.

\* Corresponding author. E-mail: mnovo@lugo.usc.es.

**Sample Preparation.** Stock solutions of PY or PB were prepared by dissolving the commercial product in water and immediately filtering to separate the impurities. The absence of fluorescent impurities in these stocks was proved by comparing the fluorescence excitation and emission spectra of diluted aqueous solutions registered at different emission and excitation wavelengths, respectively. The natural pH of these stocks was acid, in the range from 2.9 to 3.3, so that pyronine hydrolysis was very slow and the solutions were stable within 2–3 days (kept protected from light). Further acidification leads to precipitation of the pyronines. The concentrations of the stocks were estimated using the molar absorptivities found in the literature, with a value of  $\epsilon = 1.1 \times 10^5 \text{ mol}^{-1} \text{ dm}^3 \text{ cm}^{-1}$  both for PY<sup>5</sup> and for PB<sup>6</sup> at their respective absorption maxima. It must be noted that the possible inaccuracy of these values, inferred from the disagreement of the reported values, has no influence on the results obtained.

Aqueous solutions for measurements were freshly prepared by dilution of the stocks, with concentrations in the range  $(1-2) \times 10^{-5} \text{ mol dm}^{-3}$  for absorption and  $(1-3) \times 10^{-6} \text{ mol dm}^{-3}$  for fluorescence. These concentrations are low enough to avoid aggregation of the pyronines in aqueous solution. The pH of the solutions was adjusted to a constant value throughout each series in the range from 3.4 to 4.0 by adding suitable amounts of  $\text{HClO}_4$ . Samples of varying CD concentration were prepared by the addition of different volumes of a  $\beta$ -CD stock solution (concentration  $\sim 0.011 \text{ mol dm}^{-3}$ ). Poor reproducibility of absorbance and fluorescence intensity was observed for the aqueous solutions of pyronines without  $\beta$ -CD, which was attributed to the reported adsorption of pyronines on glass surfaces.<sup>6,7</sup> This problem was minimized by the addition of small amounts of  $\beta$ -CD to the pyronine stock solutions. No deoxygenation of the samples for time-resolved measurements was necessary, since these pyronines have short fluorescence lifetimes.

Solutions of the pyronines in different solvents were prepared from aliquots of the aqueous stocks, after removing water by evaporation. Absorption and fluorescence measurements were performed immediately after preparation.

**Absorption Measurements.** Absorption spectra were recorded in a Varian-Cary 300 spectrometer using quartz cells of 10.0 mm path. Baseline was recorded with water in both sample and reference cells. The important optical effect of  $\beta$ -CD on the absorption spectra was corrected using a  $\beta$ -CD solution as reference with the same concentration as the sample solution. A Haake cryostat was used to keep a constant temperature of 20 °C during the titration measurements.

**Fluorescence Measurements.** Both steady-state and time-resolved fluorescence measurements were performed with an Edinburgh Instruments F900 spectrofluorimeter, equipped with a Xenon lamp of 450 W as the excitation source for steady-state measurements and a hydrogen-filled nanosecond flashlamp for lifetime measurements using the time-correlated single photon counting technique. The hydrogen-filled flashlamp worked at a pulse frequency of 40 kHz and had a typical pulse halfwidth of 1.6 ns. Sample decays were measured at 570 nm, with completely open slits ( $\Delta\lambda \leq 20 \text{ nm}$ ). All decays were measured with a time range of 50 ns and a time resolution of 0.053 ns. Counts at the maximum were about 10 000 in all decays, also in the series with varying  $\beta$ -CD concentration, where a fixed measuring time was set. Excitation wavelengths were 515 nm for steady-state emission spectra and 310 nm in time-resolved measurements. Emission spectra were corrected for the wavelength dependence of the detection system. Excita-

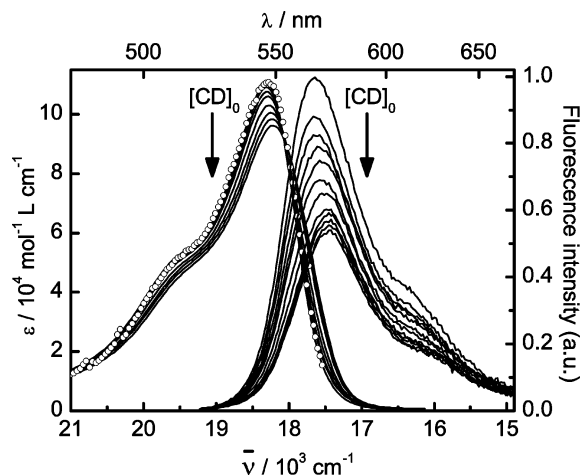


**Figure 2.** Absorption and corrected fluorescence emission spectra ( $\lambda_{\text{exc}} = 515 \text{ nm}$ ) of PY in the presence of different concentrations of  $\beta$ -CD, in the range from  $2 \times 10^{-5}$  to  $1 \times 10^{-2} \text{ mol dm}^{-3}$ . The fluorescence excitation spectrum of PY in the absence of  $\beta$ -CD registered at  $\lambda_{\text{em}} = 570 \text{ nm}$  is shown as open circles.

tion spectra were also corrected. All experiments were carried out at 20 °C.

Absolute quantum yields were determined using rhodamine B in basic ethanol as the standard, with a reported value of 0.70 for its fluorescence quantum yield.<sup>9</sup>

**Data Analysis.** The series of absorption and emission spectra recorded in the titrations with  $\beta$ -CD were analyzed using a procedure developed in our laboratory based on principal components analysis and global analysis (PCGA), which is described elsewhere.<sup>10</sup> This method can be applied to any series of spectra which vary with an external parameter, as the  $\beta$ -CD concentration in this case. The first step of PCGA is the principal components analysis (PCA), where the minimal number of spectral components responsible for the observed variations is obtained. This information helps to draw up a theoretical model which is used in the second step as a fit function for a nonlinear least-squares global analysis using the whole spectra as a data set. The results of this global fit are the physicochemical parameters involved in the model and the individual spectra of the components.

Individual fits of fluorescence decays were performed with the software package from Edinburgh Instruments, which provides deconvolution of the lamp pulse and a nonlinear least-squares fit of an exponential model to the experimental decay. The series of decays at different  $\beta$ -CD concentrations were also analyzed by a modified procedure of the above-described global analysis. This is the so-called “target” global analysis,<sup>11</sup> in which two coupled theoretical models are used, one for the time dependence and another one for the concentration dependence of the fluorescence intensity. This target fit yields directly the physicochemical parameters which describe both the time and the concentration dependence of the decays, reducing effectively the problem of parameter correlation.

## Results and Discussion

**Complexation of Pyronines Y and B with  $\beta$ -CD.** Titration experiments were performed in order to investigate the complexation ability of the pyronines with  $\beta$ -CD. Figure 2 shows the series of absorption and emission spectra of PY in the presence of different concentrations of  $\beta$ -CD. A red shift of the spectra together with a decrease in absorbance and fluorescence intensity are observed as the concentration of  $\beta$ -CD is increased. The absorption and emission spectra of PB show

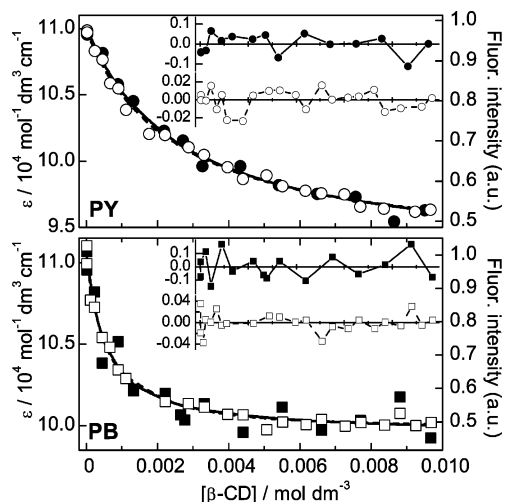


**Figure 3.** Plots of molar absorptivities at the absorption maxima (filled symbols) and fluorescence intensities at the emission maxima (open symbols) of PY and PB versus initial  $\beta$ -CD concentrations. Scales were chosen in order to show the coincidence of the variation in absorption and emission data. The lines represent the curves obtained by global fit to the experimental absorption and emission spectra. Residuals are shown as insets.

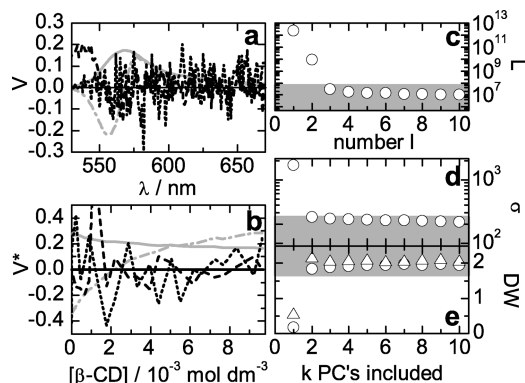


**Figure 4.** Results of PCA for the series of fluorescence emission spectra of PY with different  $\beta$ -CD concentrations shown in Figure 2: (a) the first four spectral eigenvectors in the order grey solid line, grey dash-dotted line, black dashed line, black dotted line; (b) the first four eigenvector profiles in the same order as before; (c) logarithmic plot of eigenvalues versus number of components; (d) logarithmic plot of mean error values versus number of included components; (e) plot of mean Durbin–Watson test values of residual spectra (circles) and residual profiles (triangles) versus number of included components.

analogous variations with the addition of  $\beta$ -CD, although they occur at lower  $\beta$ -CD concentrations than in the case of PY. This is shown in Figure 3, where the molar absorptivities and the fluorescence intensities at the maxima are plotted against  $\beta$ -CD concentration for the two pyronines. At a  $\beta$ -CD concentration of  $0.002 \text{ mol dm}^{-3}$ , the decrease in both absorbance and fluorescence intensity is  $\sim 90\%$  for PB, whereas it is only  $\sim 50\%$  for PY.

A clear isosbestic point is observed in the series of absorption spectra, both for PY and PB, that indicates an equilibrium between two chemical species, as it corresponds for a single complexation process. Nevertheless, the formation of two types of complexes between PY and  $\beta$ -CD with 1:1 and 1:2 stoichiometries has been proposed in the literature.<sup>7</sup> Therefore, PCA was applied to both absorption and emission data in order to find out how many species are contributing to the experimental spectra. Figure 4 shows the results of PCA for a series of emission spectra of PY in the presence of different concentrations of  $\beta$ -CD (data of Figure 2). All five statistical criteria used

in our analysis indicate that only two components are necessary to explain the systematic variations of the data: the first two eigenvectors (Figure 4a) and eigenvector profiles (Figure 4b) vary systematically, whereas the rest are random; the first two eigenvalues represent the structural variance of the data and the rest the residual variance (Figure 4c); the inclusion of two components reduces the value of the mean error down to the level of the residual mean error (Figure 4d); the mean Durbin–Watson test values calculated as a function of wavelength or as a function of  $\beta$ -CD concentration lie well above the critical value of  $\sim 1.7$  with the inclusion of the second component (Figure 4e), indicating that two components are necessary to obtain uncorrelated residuals. Moreover, the plots of residuals versus wavelength and versus  $\beta$ -CD concentration show random distributions after the inclusion of two components. Analogous results were obtained for the series of emission spectra of PB with  $\beta$ -CD, indicating that also for this pyronine two components are enough to explain the spectral variations with  $\beta$ -CD concentration. For the series of absorption spectra, two components are also obtained on the basis of eigenvector profiles, mean Durbin–Watson test values calculated as a function of  $\beta$ -CD concentration, and plots of residuals versus  $\beta$ -CD concentration. The other statistical criteria, based on the spectral profiles, are not suitable for the analysis of absorption data, since these are affected by instrumental artifacts that lead to the appearance of spurious components.<sup>10</sup>

At this point, we know that two components are involved in the variations of both absorption and emission spectra of the pyronines with  $\beta$ -CD. This means that only one type of complex of each pyronine with  $\beta$ -CD is formed, which contributes to the spectra together with the free pyronine. The simplest model to consider is a 1:1 complexation equilibrium in the ground state, defined by an association equilibrium constant ( $K$ ):



where Pyr denotes free pyronine and Pyr/CD the 1:1 complex of a pyronine with  $\beta$ -CD.

Thus, any absorption spectrum of a series is a linear combination of the individual absorption spectra of free pyronine and complex each multiplied by the corresponding equilibrium concentrations of these species. Also, emission spectra are linear combinations of the individual emission spectra of the two species and the concentration coefficients coincide with those of absorption spectra if interconversion processes do not take place at the excited state. This is the case, since the rates of association and dissociation processes are not expected to compete with the deactivation rates of the excited species. Then, on the basis of this model and under conditions of constant pyronine concentration and excess of  $\beta$ -CD ( $[\text{CD}] \approx [\text{CD}]_0$ ), the following equation is obtained that accounts for the dependence of absorbance or fluorescence intensity at a certain wavelength ( $D^\lambda$ ) on  $\beta$ -CD concentration:

$$D^\lambda = \frac{D_{\text{Pyr}}^\lambda + D_{\text{Pyr/CD}}^\lambda K[\text{CD}]_0}{1 + K[\text{CD}]_0} \quad (2)$$

where  $D_{\text{Pyr}}^\lambda$  and  $D_{\text{Pyr/CD}}^\lambda$  are the absorbances or the fluorescence intensities at  $\lambda$  when all the pyronines present were free and complexed, respectively.

Using eq 2 as a fit function, global analysis was performed for the series of absorption and emission spectra of the two pyronines with  $\beta$ -CD. The goodness of the fits is exemplified for data at certain wavelengths in Figure 3. The agreement



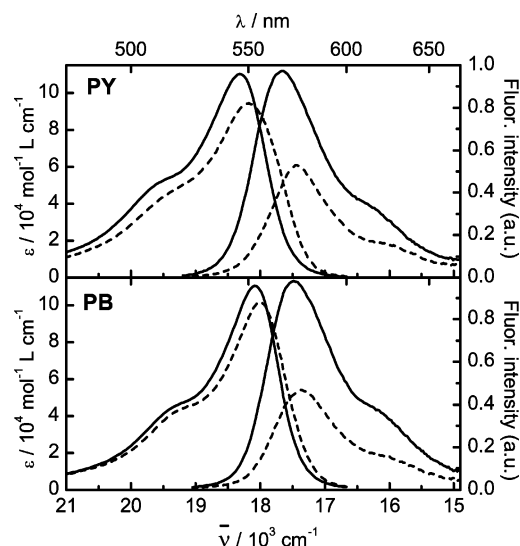


**Figure 5.** “Pure” absorption and fluorescence emission spectra of the free pyronines (solid lines) and the complexes Pyr/CD (dashed lines) obtained by global analysis of the series of absorption and emission spectra of PY and PB with different concentrations of  $\beta$ -CD.

**TABLE 1: Values of the Association Equilibrium Constants of PY and PB with  $\beta$ -CD Obtained by Global Analysis of the Series of Absorption and Emission Spectra and by Target Global Analysis of the Fluorescence Decays of Solutions with Different  $\beta$ -CD Concentrations**

$K/10^3 \text{ mol}^{-1} \text{ dm}^3$	PY	PB
absorption spectra	$0.39 \pm 0.05$	$2.0 \pm 0.4$
emission spectra	$0.40 \pm 0.04$	$2.1 \pm 0.2$
fluorescence decays	$0.36 \pm 0.03$	$2.0 \pm 0.1$

between the fitted curves and the experimental data and the random residuals indicate good fits and validate the proposed model. As a result of the global fits, the values of the association equilibrium constants were obtained (Table 1). There is very good agreement between the values determined from absorption data and those obtained from the emission spectra. This is proof that the association reaction is not a competitive process in the excited state but gives no further evidence on the occurrence of the dissociation process in the excited state. When comparing the values of the association equilibrium constants of the two pyronines, that of PB is significantly larger, indicating a stronger interaction of this pyronine with  $\beta$ -CD. This was expected in view of the stronger variations at low  $\beta$ -CD concentrations observed for PB compared to PY (Figure 3), but it is a surprising result, since it is presumed that PB would show stronger steric hindrance than PY to enter into the  $\beta$ -CD cavity. A possible explanation of this result is discussed below.

The other results of the global fits are the individual spectra of the free pyronines and the Pyr/CD complexes (Figure 5). Both the absorption and emission spectra determined for the free pyronines are in perfect accordance with the experimental spectra of the pyronines in aqueous solution, and this validates the analysis. The spectra of the complexes show red shift with respect to the free pyronines, which is more significant for the complex PY/CD. Complexation causes also a decrease in intensity, which is especially important in the emission spectra with a reduction of  $\sim 50\%$ . Further analysis of the effect of complexation on the fluorescence quantum yields of the pyronines is performed below with the aim to study the interactions between the pyronines and  $\beta$ -CD.

It is interesting to compare our results with those reported in the literature. The proposed model of 1:1 and 1:2 complexation between PY and  $\beta$ -CD<sup>7</sup> cannot be supported on the basis of

our analysis of the data with PCA. Therefore, no agreement can be expected for the association equilibrium constants and the individual absorption spectra of the complexes. In the case of PB, a single 1:1 complexation was proposed,<sup>6</sup> in accordance with our results. The reported value for the association equilibrium constant is  $\sim 2$  times higher than ours, but it is affected by a large error of 60%. The absorption spectrum proposed for the complex is qualitatively in agreement with the one determined by global analysis for PB/CD (Figure 5).

To complete the study on the complexation process, fluorescence decays of PY and PB in aqueous solutions with different concentrations of  $\beta$ -CD were measured. Table 2 shows the results of the individual fits. For PY without  $\beta$ -CD, a monoexponential decay is obtained with a lifetime of 1.76 ns, which corresponds to free PY. In the presence of  $\beta$ -CD, the decays of PY become biexponential with two constant lifetimes in the whole range of  $\beta$ -CD concentrations: one that coincides with the lifetime of free PY and another one of  $\sim 1$  ns which must be assigned to the complex of PY with  $\beta$ -CD (PY/CD). The fact that the lifetime of free pyronine does not change with the addition of  $\beta$ -CD indicates that the association reaction in the excited-state cannot compete with the deactivation processes of PY. Nevertheless, excited-state dissociation cannot be ruled out on the basis of these results, since it does not depend on  $\beta$ -CD concentration. Regarding the preexponential factors, the one corresponding to free PY decreases, whereas that of the complex increases as the  $\beta$ -CD concentration is increased (see Table 2). This is logical, since these factors are proportional to the ground-state concentrations of the two species and depend on  $\beta$ -CD concentration in the same way as absorbance or fluorescence intensity. Therefore, information about the association equilibrium constant can be extracted from the time-resolved data by performing a target global analysis of all decays simultaneously. In this analysis, a biexponential model is used to account for the time dependence of the fluorescence and a model based on the variation of the ground-state concentrations with  $\beta$ -CD concentration describes the contributions of the two species to each decay. Combining both models, the following fit function is obtained for the decays:

$$I(t, [\text{CD}]_0) = \frac{I_{\text{PYT}}}{1 + K[\text{CD}]_0} e^{-t/\tau_{\text{PYT}}} + \frac{I_{\text{PYT/CD}} K[\text{CD}]_0}{1 + K[\text{CD}]_0} e^{-t/\tau_{\text{PYT/CD}}} \quad (3)$$

where  $\tau_{\text{PYT}}$  and  $\tau_{\text{PYT/CD}}$  are the lifetimes of the free pyronine and the complex, respectively. The fit parameters  $I_{\text{PYT}}$  and  $I_{\text{PYT/CD}}$  are the fluorescence intensities at zero time when all the pyronines were free or complexed, respectively, and depend on the absorbances of the species at the excitation wavelength, their fluorescence quantum yields, and several instrumental parameters.

This model fits satisfactorily all decays. As a result of the fit, a value for the association equilibrium constant of PY with  $\beta$ -CD is obtained (Table 1), that is in good agreement with those determined from absorption and emission spectra. The fit yields also precise values for the fluorescence lifetimes of free PY and the complex PY/CD (Table 2). The lifetime of free PY is in perfect accordance with the experimental value. The lifetime of PY/CD agrees well with the values obtained in the individual fits, but it is more precise, since it is the value that better fits all the decays and it is not so much affected by the problem of parameter correlation.

The results obtained in the individual fits of PB decays are very similar to those of PY, but an additional lifetime of very small contribution is needed to obtain satisfactory fits (Table

**TABLE 2: Fluorescence Lifetimes, Amplitudes, and Chi-Square Values Obtained in the Individual Fits of a Multiexponential Model to the Fluorescence Decays of PY and PB in the Presence of Different Concentrations of  $\beta$ -CD<sup>a</sup>**

[CD] <sub>0</sub> /mM	$\tau_1$ /ns	$\tau_2$ /ns	$\tau_3$ /ns	$A_1/10^{-2}$	$A_2/10^{-2}$	$A_3/10^{-2}$	$\chi^2$
PY + $\beta$ -CD							
0		1.758 $\pm$ 0.004			100.0 $\pm$ 0.2		1.00
0.541	0.7 $\pm$ 0.2	1.77 $\pm$ 0.02		16 $\pm$ 2	84 $\pm$ 4		1.00
1.08	1.0 $\pm$ 0.2	1.78 $\pm$ 0.04		30 $\pm$ 8	70 $\pm$ 8		1.06
2.17	1.0 $\pm$ 0.1	1.74 $\pm$ 0.04		38 $\pm$ 8	62 $\pm$ 8		1.07
5.42	1.11 $\pm$ 0.02	1.76 (fixed)		64 $\pm$ 1	36 $\pm$ 2		1.12
target GA	1.08 $\pm$ 0.03	1.76 $\pm$ 0.01					
PB + $\beta$ -CD							
0		1.17 $\pm$ 0.01	2.5 $\pm$ 0.5		98 $\pm$ 2	2 $\pm$ 1	1.16
0.0201	0.15 $\pm$ 0.10	1.36 $\pm$ 0.02	2.5 (fixed)	51 $\pm$ 42	49 $\pm$ 1	< 1	1.06
0.570	0.40 $\pm$ 0.09	1.23 $\pm$ 0.07	3.0 $\pm$ 0.8	51 $\pm$ 5	49 $\pm$ 4	1 $\pm$ 1	1.21
1.12	0.35 $\pm$ 0.09	1.10 $\pm$ 0.07	2.7 $\pm$ 0.5	55 $\pm$ 5	45 $\pm$ 5	1 $\pm$ 1	1.08
2.22	0.44 $\pm$ 0.03	1.15 (fixed)	2.5 $\pm$ 0.4	73 $\pm$ 2	27 $\pm$ 2	1.0 $\pm$ 0.5	1.17
5.52	0.45 $\pm$ 0.06	1.1 $\pm$ 0.1	3.5 $\pm$ 0.5	77 $\pm$ 5	23 $\pm$ 8	1.0 $\pm$ 0.3	1.23
target GA	0.50 $\pm$ 0.05	1.25 $\pm$ 0.02	3 (fixed)				

<sup>a</sup> The sum of amplitudes has been normalized to unity to facilitate comparison.  $\lambda_{\text{exc}} = 310$  nm, and  $\lambda_{\text{em}} = 570$  nm. The values of the fluorescence lifetimes obtained by target global analysis of the decays are also given.

2). In the absence of  $\beta$ -CD, the main lifetime of 1.17 ns is due to free PB and the residual lifetime of  $\sim 2.5$  ns must be attributed to an impurity. This could be the xanthinol formed by the hydrolysis of PB, which would be detectable in time-resolved measurements because of the excitation wavelength used. Such a species is not observed in the decays of PY, since this pyronine reacts more slowly than PB.<sup>5</sup> The decays of PB with different  $\beta$ -CD concentrations show all the small contribution attributed to the xanthinol and two main lifetimes, one which coincides well with the lifetime of free PB and another of  $\sim 0.4$  ns. The interpretation is the same as that for PY: the shortest lifetime is due to the complex PB/CD, and therefore, its contribution increases with  $\beta$ -CD concentration, whereas the contribution of free PB decreases. To check this interpretation, a target global analysis was performed, where the fit function was that given by eq 3 with an additional exponential term which accounts for the contribution of the impurity and is independent of  $\beta$ -CD concentration. This model fits satisfactorily to all decays and yields a value of the association equilibrium constant which is in very good agreement with those determined from absorption and emission spectra (Table 1). Also, precise values of the fluorescence lifetimes are obtained, with that of free PB being in quite good agreement with the experimental value (Table 2). The resulting lifetime of the complex PB/CD is slightly higher than the values obtained in the individual fits but agrees within the errors. As in the case of PY, complexation of PB by  $\beta$ -CD causes an important decrease in lifetime, which matches the decrease in fluorescence quantum yield. A possible explanation for these variations will be discussed below.

**Analysis of the Interactions between Pyronines Y and B and  $\beta$ -CD.** The pyronines under study show an opposite behavior to that of most fluorophores when included in CD cavities, since their fluorescence quantum yields and lifetimes decrease instead of increase by complexation. This has also been observed in other substrates, as for example the parent molecule acridine, and specific guest–host interactions have been proposed to explain this atypical behavior.<sup>12</sup> To analyze these effects of the complexation, the photophysical properties of the Pyr/CD complexes will be compared with those of the pyronines in different solvents. The solvents were chosen among those which dissolve these pyronines to cover a wide range of polarity in terms of the empirical parameter  $E_T(30)$ .<sup>13</sup> Absorption and emission spectra and fluorescence lifetimes were measured for the two pyronines in the selected solvents.

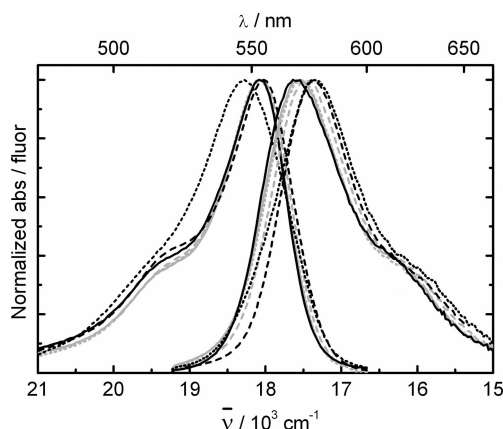


**Figure 6.** Absorption and corrected fluorescence emission spectra of PB in different solvents: water (black solid line), ethanol (grey solid line), acetonitrile (grey dotted line), acetone (grey dashed line), dioxane (black dotted line) and the complex PB/CD (black dashed line).  $\lambda_{\text{exc}} = 515$  nm.

Figure 6 shows the experimental absorption and emission spectra of PB in the different solvents and those of the complex PB/CD obtained before (see Figure 5). The spectra, which were normalized at their maxima to allow comparison, show small shifts with the change of the solvent. A slight red shift of the PB absorption spectrum is observed as solvent polarity is decreased, except for dioxane, where the low-energy side of the band shifts to the red, whereas the maximum goes to higher energies. The absorption spectrum of the PB/CD complex is the most red-shifted and coincides with that in dioxane at lower energies. The PB emission spectrum shifts also to lower energies with decreasing solvent polarity, and the effect is more pronounced than that for absorption. The emission spectrum of the complex PB/CD is very similar to that of PB in dioxane, except for the shoulder of the latter at the high-energy side of the band. Analogous results were obtained for PY in the different solvents. To further analyze this effect, the emission maxima of the pyronines were plotted against the empirical polarity parameter  $E_T(30)$  (Figure 7a). No linear correlation is obtained, as would be expected for a general polarity effect of the solvent. This indicates that specific interactions are responsible for the spectral shift observed. The emission maxima of the complexes are very similar to those of the pyronines in dioxane, so that analogous environments for the pyronines can be expected in the two media. Nevertheless, the spectra of the complexes do

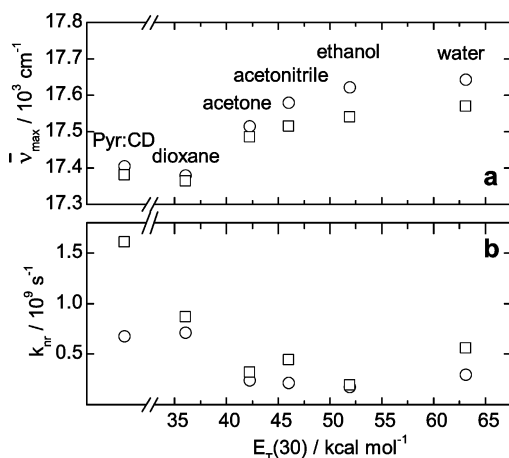


**Figure 7.** (a) Plot of the maximal emission wavenumbers of PY (circles) and PB (squares) in different solvents and in the Pyr/CD complexes versus the empirical polarity parameter  $E_T(30)$ . (b) Plot of the nonradiative deactivation rate constants of PY (circles) and PB (squares) in different solvents and in the Pyr/CD complexes versus  $E_T(30)$ .

**TABLE 3: Fluorescence Lifetimes, Amplitudes, and Chi-Square Values Obtained in the Fits of a Biexponential Model to the Fluorescence Decays of PY and PB in Different Solvents.  $\lambda_{\text{exc}} = 310 \text{ nm}$ , and  $\lambda_{\text{em}} = 570 \text{ nm}$**

Pyr/solvent	$\tau_1/\text{ns}$	$\tau_2/\text{ns}$	$A_1/10^{-3}$	$A_2/10^{-3}$	$\chi^2$
PY/ethanol	$2.18 \pm 0.01$	$5.8 \pm 0.7$	39.0	<1	1.19
PY/acetonitrile	$1.851 \pm 0.008$	$7 \pm 2$	44.0	<1	1.07
PY/acetone	$1.94 \pm 0.03$	3.4 (fixed)	6.0	<1	1.16
PY/1,4-dioxane	$1.03 \pm 0.03$	$3.4 \pm 0.1$	54.0	5	1.21
PB/ethanol	$1.71 \pm 0.04$	$2.7 \pm 0.6$	50	3	1.02
PB/acetonitrile	$1.24 \pm 0.01$	$3.6 \pm 0.9$	65.0	<1	1.04
PB/acetone	$1.52 \pm 0.02$	3.5 (fixed)	51.0	4	1.25
PB/1,4-dioxane	$0.92 \pm 0.03$	$3.45 \pm 0.04$	41	19	1.34

not show the anomalous emission shoulder and the blue shift of the absorption maxima observed for these pyronines in dioxane (see Figure 6). These effects may be due to aggregation of the pyronines in this solvent. Schiller et al. showed that dimerization of these pyronines leads to a strong blue shift of their absorption maxima,<sup>6,7</sup> very similar to that observed in dioxane. Moreover, it is known that specific solvent interactions play an important role in the formation of aggregates by xanthene dyes.<sup>14</sup> The fact that no aggregation effect is observed in the spectra of the complexes can be understood, since a pyronine dimer would not fit into the  $\beta$ -CD cavity.

The most important effect of the solvent is the variation in the fluorescence lifetimes of the pyronines and in their fluorescence quantum yields. Table 3 shows the values of the fluorescence lifetimes of PY and PB in the different solvents. Biexponential decays are obtained in all cases, with a main lifetime ranging from 0.9 to 2.2 ns due to the pyronine and a longer residual lifetime. The contribution of this second lifetime is very small, especially for PY, so that it can be attributed to the xanthidrol obtained by hydrolysis or to an analogous product resulting from the nucleophilic attack of the solvent molecules at the C9 position of the pyronine. With respect to water (see Table 2), the lifetimes of PY and PB in ethanol, acetonitrile, and acetone increase between 5 and 45%, with the higher variation corresponding to ethanol. On the contrary, in dioxane, there is a significant decrease of the fluorescence lifetime of  $\sim 40\%$  for PY and  $\sim 20\%$  for PB. The lifetime of PY in dioxane coincides with that of the complex PY/CD (Table 2), whereas the lifetime of the complex PB/CD is shorter than that of PB in dioxane. Analogous variations are observed in the fluorescence

**TABLE 4: Fluorescence Quantum Yields, Radiative Deactivation Rate Constants, and Nonradiative Deactivation Rate Constants of PY and PB in Different Solvents and in the Complexes PY/CD and PB/CD**

Pyr/solvent	$\phi$	$k_r/10^9 \text{ s}^{-1}$	$k_{\text{nr}}/10^9 \text{ s}^{-1}$
PY/water	0.47	0.27	0.30
PY/ethanol	0.61	0.28	0.18
PY/acetonitrile	0.60	0.32	0.22
PY/acetone	0.53	0.27	0.24
PY/1,4-dioxane	0.26	0.26	0.71
PY/CD complex	0.27	0.25	0.68
PB/water	0.36	0.31	0.56
PB/ethanol	0.65	0.36	0.20
PB/acetonitrile	0.44	0.35	0.44
PB/acetone	0.50	0.33	0.33
PB/1,4-dioxane	0.18	0.19	0.87
PB/CD complex	0.19	0.38	1.6

quantum yields (Table 4), with increases between 13 and 81% in ethanol, acetonitrile, and acetone and decreases around 50% in dioxane with respect to water. Again, the quantum yields of the complexes Pyr/CD coincide well with those in dioxane, indicating the similarities in the microenvironment of the pyronines in the two media. This result can be understood, since the glucosidic oxygens that point to the interior of the CD cavity are ether-type oxygens as those in dioxane, so that in both cases the pyronines would be surrounded by an electron-rich environment.

Further analysis of these solvent effects implies determination of the deactivation rate constants. Radiative and nonradiative deactivation rate constants of the pyronines in the different solvents and in the complexes were calculated from the fluorescence lifetimes and quantum yields (Table 4). The values obtained for the radiative rate constants are in very good agreement with those calculated from the absorption and emission spectra using the theoretical equations of Förster<sup>15</sup> and Strickler and Berg,<sup>16</sup> proving consistency of results. It can be seen that the radiative deactivation constants have similar values in all solvents for both pyronines. This could be expected, since the radiative deactivation constant is usually not very solvent dependent. On the contrary, differences are observed in the nonradiative deactivation constants. Values between 0.18 and  $0.30 \text{ ns}^{-1}$  are obtained for PY in water, ethanol, acetonitrile, and acetone, whereas PY in dioxane and the complex PY/CD show threefold nonradiative rate constants. For PB in the first mentioned solvents, the values of  $k_{\text{nr}}$  vary between 0.20 and  $0.56 \text{ ns}^{-1}$  and are in accordance with the reported values for ethanol and water.<sup>17</sup> As for PY, this rate constant increases significantly in dioxane. The increase is even larger for the complex PB/CD, with a value of  $k_{\text{nr}}$  of about twice that in dioxane. Figure 7b shows the variation of  $k_{\text{nr}}$  with the parameter  $E_T(30)$ . No correlation can be found of  $k_{\text{nr}}$  with solvent polarity. The values of  $k_{\text{nr}}$  are roughly constant in the four other polar solvents, especially for PY, and the only significant variations are observed for both pyronines in dioxane and inside the  $\beta$ -CD cavity. These results suggest again the existence of specific interactions of the pyronines with the electron-rich oxygens present in those media.

Now a mechanism must be proposed in order to explain the observed solvent effects on the photophysical properties of the pyronines. The effect of solvent on the nonradiative deactivation of rhodamines has been extensively studied, and different mechanisms have been proposed as pathways for deactivation, where charge transfer from the amino groups to the xanthene moiety and hydrogen-bond interactions with the solvent molecules play important roles.<sup>9,18</sup> Analogous models were used to explain the behavior of PB in polar protic and aprotic



solvents.<sup>17,19</sup> In these works, a two-state mechanism is proposed, where a fluorescent planar state is in rapid equilibrium with a nonemissive nonplanar state, whose energy is affected by solvent polarity, leading to the observed variations of  $k_{nr}$ . Nevertheless, the reported solvent effects are not so important as those determined for the pyronines in dioxane and in the Pyr/CD complexes.

Taking into account all of these models, the following interpretation is proposed for our results. A nonemissive charge-transfer (CT) excited state of the pyronines is formed where the positive charge is located at the xanthene ring (as in the resonance structures on the right in Figure 1), and a structural change of the amino groups takes place. This could be a TICT state, but our data do not give any evidence for or against the rotation about the xanthene–amine bond. Fluorescence emission comes from the locally excited state and is slightly affected by solvent polarity, explaining the small spectral shift of the emission band. Nonradiative deactivation occurs via the CT state and is very much determined by the ability of the solvent to stabilize this state. In the cases of dioxane and of the CD cavity, the high electron density due to the ether-type oxygens would provide an effective stabilization of the positively charged xanthene, favoring the formation of the CT state. It has been shown that the glucosidic oxygens in  $\beta$ -CD are almost coplanar and centered in the middle of the cavity,<sup>20</sup> so that their location is most suitable for interaction with the central atoms of the xanthene ring. Moreover, since the xanthene moiety fits completely into the  $\beta$ -CD cavity, it could be expected that the amino groups of the pyronines form hydrogen bonds with the hydroxyl groups on the outer rims of the CD, contributing to the stabilization of the CT state. The fact that the value of  $k_{nr}$  for the complex PB/CD is much higher than that of PB in dioxane and that of the complex PY/CD shows that the CT state is especially stable in the PB/CD complex. This seems to be a large effect for the substitution of the methyl groups in PY by ethyl groups in PB. Nevertheless, such an effect on the stabilization of the CT state has been observed in other molecules which exhibit emission from that CT state. That is the case for the extensively studied molecule *p*-dimethylaminobenzonitrile and its higher dialkyl homologues, where emission of the CT state increases significantly with the length of the alkyl chain.<sup>21</sup> Also, an important effect of alkylation on the nonradiative deactivation of rhodamines has been observed.<sup>18</sup>

Above, we proposed the specific interactions between the pyronines and the electron-rich oxygens in dioxane and in the CD cavity as an explanation for the photophysical behavior of the pyronines in the excited state. This hypothesis could also explain the different stability of the ground-state complexes

formed by the two pyronines, which manifests in the 5-fold larger association equilibrium constant of PB with respect to PY (Table I). From the values of  $k_{nr}$ , it was deduced that PB interacts stronger than PY with  $\beta$ -CD, leading to a larger stabilization of the CT state in that molecule. The experimental work with PB shows that this pyronine has much higher reactivity with water than PY, indicating a more pronounced charge defect at the C9 position of the xanthene ring in PB. This suggests that the ground-state electronic distribution of PB has an important contribution of the carbocation resonance structure (Figure 1) and hence it would be effectively stabilized by the electron-rich oxygens present in the CD cavity.

**Acknowledgment.** This work has been supported by the Ministerio de Ciencia y Tecnología (Project MAT2001-2911). Belén Reija thanks the Ministerio de Educación y Ciencia for a research scholarship.

## References and Notes

- (1) Szejtli, J.; Osa, T.; Atwood, J. L. *Cyclodextrins. Comprehensive Supramolecular Chemistry*; Pergamon: Oxford, U.K., 1996; Vol. 3.
- (2) Fujiji, K.; Iwanaga, C.; Koizumi, M. *Bull. Chem. Soc. Jpn.* **1962**, 35, 185.
- (3) Gianneschi, L. P.; Kurucsev, T. *J. Chem. Soc., Faraday Trans. 2* **1974**, 70, 1334.
- (4) Gianneschi, L. P.; Cant, A.; Kurucsev, T. *J. Chem. Soc., Faraday Trans. 2* **1977**, 73, 664.
- (5) Baraka, M. E.; Deumie, M.; Viallet, P.; Lampidis, T. J. *J. Photochem. Photobiol., A* **1991**, 56, 295.
- (6) Schiller, R. L.; Lincoln, S. F.; Coates, J. H. *J. Chem. Soc., Faraday Trans. 1* **1986**, 82, 2123.
- (7) Schiller, R. L.; Lincoln, S. F.; Coates, J. H. *J. Chem. Soc., Faraday Trans. 1* **1987**, 83, 3237.
- (8) Schiller, R. L.; Lincoln, S. F.; Coates, J. H. *J. Inclusion Phenom. Macrocyclic Chem.* **1987**, 5, 59.
- (9) López Arbeloa, F.; López Arbeloa, T.; Tapia Estévez, M. J.; López Arbeloa, I. *J. Phys. Chem.* **1991**, 95, 2203.
- (10) Al-Soufi, W.; Novo, M.; Mosquera, M. *Appl. Spectrosc.* **2001**, 55, 630.
- (11) Beechem, J. M. *Methods Enzymol.* **1992**, 210, 37.
- (12) Bortolus, P.; Monti, S. *Adv. Photochem.* **1996**, 21, 1.
- (13) Reichardt, C. *Solvents and solvent effects in organic chemistry*; Wiley-VCH: Weinheim, Germany, 2003.
- (14) Valdes-Aguilera, O.; Neckers, D. C. *Acc. Chem. Res.* **1989**, 22, 171.
- (15) Ferrante, C.; Kensity, U.; Dick, B. *J. Phys. Chem.* **1993**, 97, 13457.
- (16) Strickler, S. J.; Berg, R. A. *J. Chem. Phys.* **1962**, 37, 814.
- (17) Onganer, Y.; Quitevis, E. L. *J. Phys. Chem.* **1992**, 96, 7996.
- (18) López Arbeloa, T.; López Arbeloa, F.; Hernández Bartolome, P.; López Arbeloa, I. *Chem. Phys.* **1992**, 160, 123.
- (19) Acemioğlu, B.; Arik, M.; Onganer, Y. *J. Lumin.* **2002**, 97, 153.
- (20) Saenger, W.; Jacob, J.; Gessler, K.; Steiner, T.; Hoffmann, D.; Sanbe, H.; Koizumi, K.; Smith, S. M.; Takaha, T. *Chem. Rev.* **1998**, 98, 1787.
- (21) Grabowski, Z. R.; Rotkiewicz, K.; Rettig, W. *Chem. Rev.* **2003**, 103, 3899.